Diagn Interv Radiol 2024; DOI: 10.4274/dir.2024.232460

ABDOMINAL IMAGING

ORIGINAL ARTICLE

Value of perfusion parameters from golden-angle radial sparse parallel dynamic contrast-enhanced magnetic resonance imaging in predicting pathological complete response after neoadjuvant chemoradiotherapy for locally advanced rectal cancer

Yu-Ning Pan[1,2]
Meng-Yin Gu[3]
Quan-Liang Mao[2]
Yu-Guo Wei[4]
Lin Zhang[1]
Guang-Yu Tang[1]

[1]Shanghai Tenth People's Hospital of Tongji University, Department of Radiology, Shanghai, China

[2]The First Affiliated Hospital of Ningbo University, Department of Radiology, Ningbo, China

[3]Ningbo University, Department of Medical College, Ningbo, China

[4]GE Healthcare, Global Medical Service, Advanced Analytics, Hangzhou, China

Corresponding authors: Lin Zhang, Guang-Yu Tang

E-mail: lynn122500@hotmail.com, tgy17@tongji.edu.cn

Received 18 August 2023; revision requested 13 September 2023; last revision received 05 February 2024; accepted 10 February 2024.

Epub: 18.03.2024

Publication date: xx.xx.2024

DOI: 10.4274/dir.2024.232460

PURPOSE

Non-invasive methods for predicting pathological complete response (pCR) after neoadjuvant chemoradiotherapy (nCRT) can provide distinct leverage in the management of patients with locally advanced rectal cancer (LARC). This study aimed to investigate whether including the golden-angle radial sparse parallel (GRASP) dynamic contrast-enhanced magnetic resonance imaging (DCE-MRI) perfusion parameter (K_{trans}), in addition to tumor regression grading (TRG) and apparent diffusion coefficient (ADC) values, can improve the predictive ability for pCR.

METHODS

Patients with LARC who underwent nCRT and subsequent surgery were included. The imaging parameters were compared between patients with and without pCR. Receiver operating characteristic (ROC) curve analysis was used to evaluate the predictive ability of these parameters for pCR.

RESULTS

A total of 111 patients were included in the study. A pCR was obtained in 32 patients (28.8%). MRI-based TRG (mrTRG) showed a negative correlation with pCR ($r = -0.61$, $P < 0.001$), and the average ADC value showed a positive correlation with pCR ($r = 0.62$, $P < 0.001$). Before nCRT, K_{trans} in the pCR group was significantly higher than in the non-pCR group (1.30 ± 0.24 vs. 0.88 ± 0.34, $P < 0.001$), but no difference was identified after nCRT. Following ROC curve analysis, the area under the curve (AUC) of mrTRG (level 1–2), average ADC value, and K_{trans} value for predicting pCR were 0.738 [95% confidence interval (CI): 0.65–0.82], 0.78 (95% CI: 0.69–0.86), and 0.84 (95% CI: 0.77–0.92), respectively. The model combining the three parameters had significantly higher predictive ability for pCR (AUC: 0.94, 95% CI: 0.88–0.98).

CONCLUSION

The use of a combination of the GRASP DCE-MRI K_{trans} with mrTRG and ADC can lead to a better pCR predictive performance.

KEYWORDS

Rectal cancer, locally advanced, magnetic resonance imaging, neoadjuvant chemoradiotherapy, tumor regression grading, complete response

The prevalence of colorectal cancer is projected to rise by 60% in 2030,[1] with morbidity and mortality rates rapidly increasing in many low- and middle-income countries. Rectal cancer (RC) accounts for approximately 30% of all cases of colorectal cancer.[2] Neoadjuvant chemoradiotherapy (nCRT) followed by total mesorectal excision is the standard treatment for locally advanced RC (LARC).[3]

You may cite this article as: Pan YN, Gu MY, Mao QL, Wei YG, Zhang L, Tang GY. Value of perfusion parameters from golden-angle radial sparse parallel dynamic contrast-enhanced magnetic resonance imaging in predicting pathological complete response after neoadjuvant chemoradiotherapy for locally advanced rectal cancer. *Diagn Interv Radiol.* 18 March 2024 DOI: 10.4274/dir.2024.232460 [Epub Ahead of Print].

Approximately 50%–60% of patients with LARC experience tumor regression after nCRT, and 15%–30% of these patients achieve pathological complete response (pCR),[4] which is defined as the absence of cancer cells in the surgically resected samples. Therefore, the pathological stage for a pCR specimen is T0 N0 M0.[5] Achievement of pCR does not guarantee long-term survival;[6,7] however, the local recurrence rate and distant metastasis rate of patients achieving pCR are lower than those of patients not achieving pCR, and the 5-year survival rate is higher than that of patients who do not achieve pCR.[4,8] Therefore, pCR has remained the objective of nCRT.

The optimal treatment approach for patients who achieve pCR after nCRT is an important issue. Instead of the traditional radical surgery, some surgeons recommend non-operative treatment to avoid these complications.[7-9] Before choosing the therapeutic method, it is crucial to develop an accurate and non-invasive strategy for identifying individuals who could have a pCR.

Rectal magnetic resonance imaging (MRI) has become the standard method to evaluate the efficacy of nCRT in the treatment of LARC. In 2011, Patel et al.[10] proposed tumor regression grading (TRG) based on the proportion of lesion fibrosis and residual tumor on MRI (mrTRG). However, the traditional morphological qualitative assessment based on a T2-weighted (T2W) sequence has suboptimal performance in observing and distinguishing residual tumors and treatment-related changes. As a result, radiologists may over-stage the tumor after nCRT,[11] particularly since it is not effective in predicting pCR,[12] and the diagnostic accuracy is approximately 50%.[13]

Main points

- A non-invasive method to identify individuals who achieved a pathological complete response (pCR) after neoadjuvant chemoradiotherapy (nCRT) is important to avoid excessive medical treatment.
- The value of golden-angle radial sparse parallel (GRASP) dynamic contrast-enhanced magnetic resonance imaging (DCE-MRI) in predicting the therapeutic effect of nCRT in tumors is still controversial.
- By comparing with final pathological outcomes, the diagnostic accuracy of imaging parameters obtained from GRASP DCE-MRI was assessed.
- Combining the GRASP DCE-MRI perfusion parameter value with tumor regression grading and apparent diffusion coefficient values can lead to a better pCR predictive performance.

Recently, there has been a need for integrating multiple imaging evaluation methods to enable a more comprehensive characterization of tumor biology and therapeutic response.[14] Dynamic contrast-enhanced MRI (DCE-MRI) can reflect blood vessel permeability by displaying hemodynamic changes and can enable an assessment of tissue perfusion and oxygen levels at the macro level.[15] However, due to the influence of respiratory movement and temporal resolution, its value in predicting the therapeutic effect of nCRT in tumors is still controversial.[16-18] The golden-angle radial sparse parallel (GRASP) MRI sequence has recently been applied in clinical settings. This technique integrates the advantages of StarVIBE and TWISTIBE sequences and combines motion-insensitive, golden-angle, star-stacked acquisition and compressed sensing reconstruction to improve temporal resolution. The artifacts caused by patient and intestinal motion are reduced by radial acquisition.[19] The GRASP technique has been shown to have high accuracy in imaging motion-sensitive organs such as kidneys, liver, and prostate,[20-22] as well as the rectum.[19] However, the use of GRASP DCE-MRI perfusion parameters (K_{trans}) to predict pCR has not yet been investigated.

This study investigated whether the additional GRASP DCE-MRI K_{trans} value, based on the mrTRG and apparent diffusion coefficient (ADC) values of T2W imaging (T2WI), can enable a more accurate prediction of pCR after nCRT for LARC.

Methods

Study population

This was a retrospective study. The study protocol was approved by the Ethics Committee of The First Affiliated Hospital of Ningbo University (approval number: 2022-R01025). The informed consent of patients was waived due to the nature of the study. Clinicopathologic data of patients with RC who were admitted to the hospital between January 2020 and August 2022 were retrospectively analyzed. The inclusion criteria were as follows: (1) RC was pathologically confirmed by colonoscopy, and LARC was confirmed by preoperative MRI (cT3-4 and/or cN+), and all patients underwent nCRT followed by radical total mesorectal resection; (2) the distal margin of the lesion was <12 cm from the anus; (3) there were no distant metastases. The exclusion criteria were as follows: (1) incomplete nCRT; (2) total mesorectal excision was not performed; (3) the time interval from nCRT to operation was >16 weeks; (4) there was a lack of complete MRI or postoperative pathological data.

Neoadjuvant chemotherapy protocol

All patients received conventional long-term concurrent chemoradiotherapy. Gross tumor volume included the primary rectal mass and metastatic lymph nodes, and clinical target volume included the mesenteric region, anterior sacral lymph nodes, internal iliac lymph nodes, and obturator lymph node drainage area. External iliac lymph nodes were irradiated if T4 tumors invaded the anterior structures (male prostate or female vagina) and/or obturator lymph node metastasis occurred. The total dose of radiation was 45.5–50.4 Gy (25–28 times), and the single dose was 1.8–2.0 Gy. Radiotherapy was administered in combination with oral capecitabine (825 mg/m^2) twice a day. One cycle of XELOX (capecitabine and oxaliplatin) consolidation chemotherapy was administered 3–4 weeks after the completion of radiotherapy. Radical surgery was performed 8–12 weeks after radiotherapy.

Magnetic resonance imaging examinations

All patients underwent MRI examinations twice. The first examination was 1 week before nCRT, and the second examination was 8 weeks after nCRT. A Siemens Vida 3.0 T scanner (Erlangen, Germany) and 16-channel abdominal coil were applied. The patient was placed in the supine position, and the foot was scanned first. Scanning protocols included high-resolution T2WI, diffusion-weighted imaging (DWI), and GRASP DCE-MRI. Scanning directions included axial, coronal, sagittal, and oblique planes (Table 1). The GRASP DCE-MRI contrast agent was Gd-DTPA (0.1 mmol/kg, 2 mL/s, Hengrui Medicine), and a star K-space trajectory of a golden-angle stack using a 3D gradient echo sequence was implemented. The minimum sampling time was 150 s, and a total of 1,586 radial spokes were obtained consecutively within an interval of 185 s.

Tumor regression grading

Pathologic TRG (pTRG) grading was performed according to the criteria proposed by Mandard et al.[23], as follows: pTRG0 (pCR): no tumor cells; pTRG1: single or small clusters of tumor cells; pTRG2: fibrosis more than tumor residual; pTRG3: fibrosis less than tumor residual; pTRG4: free of fibrosis with extensive tumor residue.

Image analysis

All image analyses and measurements were performed at the post-processing workstation (Siemens, Germany) using the measurement tools provided by the workstation. Measurements of ADC values and DCE-MRI parameters were performed by two senior radiologists (YN Pan and L Zhang) with more than 10 years of experience in this field. The radiologists selected three regions of interest (ROIs) in the plane of maximum tumor size on the original T2W image. The same ROI was then automatically overlaid on the DWI, ADC, and GRASP DCE-MRI K_{trans} images. Each ROI had an area ≥4 mm^2. The average value of the three ROI areas was taken as the final result. When obtaining the ROI, the intestinal lumen, artifacts, and blood vessels were not included. Notably, the radiologists who performed the ROI measurements were blinded to the pathological outcomes to minimize the likelihood of selection bias during the analysis. If the boundary of the residual tumor could not be determined clearly, the ROI was placed in the region corresponding to the tumor area before nCRT. Since the ADC map had fewer pixels and the ROI area after treatment was small, only the ADC_{mean} obtained from the ROI placement was calculated. In accordance with the Mercury Group's definition,[10] the mrTRG grading was performed on post-treatment T2WI images. Subsequently, mrTRG grading was performed using the following criteria: grade 1-linear or crescent-shaped body, mucosa or submucosa with a 1–2 mm scar or rectum wall clearly normalized; grade 2-dense fibrosis, no significant residual tumor; grade 3-more than 50% fibrosis or mucous, residual tumor signals can be seen; grade 4-small areas of fibrosis or mucus, but mostly tumors; grade 5-identical in appearance to the primary tumor or tumor progression. The mrTRG grades 1 and 2 were defined as a clinically complete response (cCR) (Figure 1). All scanned images were transferred to a Siemens workstation running syngo.via for post-processing. The Tofts two-compartment model was used for the calculation. The artery input function was selected in "fast" mode to obtain permeability-related parameters in the ROI through measurements. These parameters included the volume transfer constant (K_{trans}), extracellular extravascular space volume fraction (V_e), and rate constant (K_{ep}). Pre-treatment values of these parameters were utilized as primary measures.

Statistical analysis

The SPSS 22.0 and R (4.1.3) software packages were used for statistical analyses. Student's t-test and the Wilcoxon rank sum test were used to compare the values of ADC, mrTRG, K_{trans}, K_{ep}, and V_e between patients with and without pCR after nCRT. The intraclass correlation coefficient (ICC) was used to assess the consistency between the two radiologists in evaluating the various parameters. Receiver operating characteristic (ROC) curve analysis was performed to evaluate the predictive value of the cCR (mrTRG1–2 level), average ADC value, and pre-nCRT K_{trans} value for pCR. The optimal threshold was determined by the Youden index, and the sensitivity, specificity, positive predictive value, and negative predictive value were calculated. Multivariate logistic regression was used to construct a model to predict pCR with backward stepwise selection. The Delong test was used to analyze the difference in diagnostic performance among ROC curves, and *P* values of <0.05 were considered indicative of statistical significance.

Table 1. Patient characteristics and pathological outcomes of the study cohort

	Overall (n = 111)	pCR (n = 32)	Non-pCR (n = 79)	*P* value
Age (years) ± SD	62.3 ± 10.6	62.9 ± 9.6	61.8 ± 11.2	0.49
Sex, n				
M	66	19	47	0.35
F	45	13	32	
The pathological types, n				
Canalicular adenocarcinoma	81	23	58	0.37
Papillary adenocarcinoma	19	5	14	
Mucinous adenocarcinoma	11	4	7	
Tumor differentiation, n				
Well-differentiated	21	13	8	0.03
Moderately differentiated	68	15	53	
Poorly differentiated	22	4	18	

SD, standard deviation; pCR, pathological complete response; M, male; F, female.

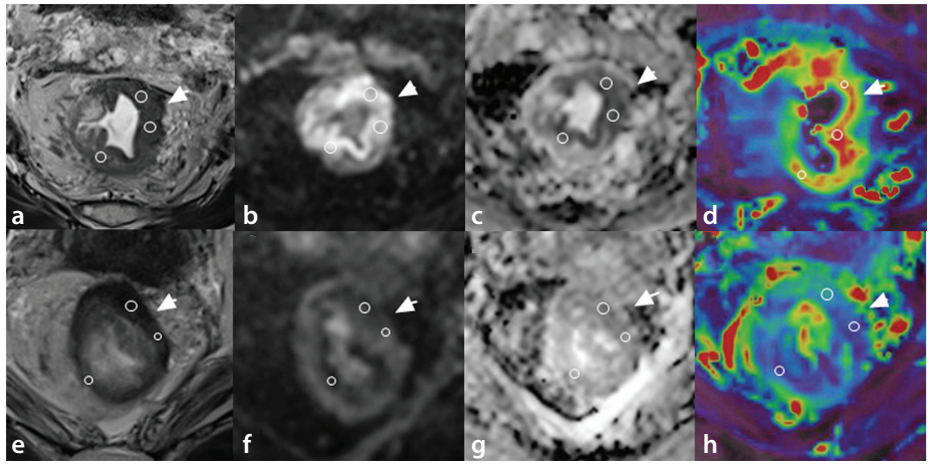

Figure 1. Magnetic resonance imaging of a 68-year-old patient with rectal cancer who underwent neoadjuvant chemoradiotherapy (nCRT) and postoperative pathological specimen identified achievement of complete response. **(a)** Before treatment, the tumor was mainly located on the left side, involving 3/4 perimeter of the rectum, and the outer membrane was involved (cT3N0, white arrow). **(b)** Before treatment, the tumor area was significantly limited in diffusion (white arrow). **(c)** Apparent diffusion coefficient (ADC) image before treatment showed a low signal in the tumor area (white arrow). **(d)** Golden-angle radial sparse parallel dynamic contrast-enhanced magnetic resonance imaging (GRASP DCE-MRI) perfusion parameter (K_{trans}) image: the tumor area is dominated by high signals with red on presentations (white arrow). **(e)** The mass was significantly reduced and fibrotic after nCRT (white arrow). **(f)** After nCRT, the diffusion restriction on the diffusion-weighted imaging disappeared, leaving only a few high signal areas (white arrow). **(g)** No obvious low signal area was found in ADC values after nCRT (white arrow). **(h)** GRASP DCE-MRI K_{trans} image; the tumor area is dominated by a blue signal (white arrow).

Results

Baseline characteristics

A total of 285 patients with RC were admitted during the study reference period. Of

these, 111 patients (45 women, 66 men, mean age: 62.3 ± 10.6 years) met the criteria for inclusion in the study. The patient selection flowchart is shown in Figure 2. The distribution of pathological types in the cohort was as follows: 81 cases of canalicular adenocarcinoma, 19 cases of papillary adenocarcinoma, and 11 cases of mucinous adenocarcinoma. Of the 111 cases, 21 were well-differentiated, 68 were moderately differentiated, and 22 were poorly differentiated. According to postoperative pathological specimens, pCR was achieved in 32 cases (28.8%).

Results of imaging evaluation

The grade of tumor regression was evaluated on T2WI. Five patients had mrTRG grade 1, 18 patients had mrTRG grade 2, 68 patients had mrTRG grade 3, 17 patients had mrTRG grade 4, and 3 patients had mrTRG grade 5. In total, 23 patients (20.7%) experienced cCR.

Post-treatment ADC values ranged from (0.83 ± 0.12) × 10^{-3} mm^2 to (2.6 ± 0.25) × 10^{-3} mm^2. After nCRT, the values of K_{trans} (0.96 ± 0.40 vs. 0.44 ± 0.25, $P < 0.001$) and K_{ep} (0.69 ± 0.54 vs. 0.55 ± 0.38, $P = 0.02$) were both significantly decreased in all patients. However, V_e showed no significant decrease after treatment (0.59 ± 0.36 vs. 0.54 ± 0.26, $P = 0.12$) (Table 2).

The two radiologists showed good consistency in evaluating mrTRG (ICC: 0.81, 95% CI: 0.77–0.88), ADC (ICC: 0.86, 95% CI: 0.84–0.97), K_{trans} (ICC: 0.88, 95% CI: 0.76–0.87), K_{ep} values (ICC: 0.68, 95% CI: 0.62–0.78), and V_e (ICC: 0.69, 95% CI: 0.63–0.76).

Correlation between imaging evaluation parameters and pathological outcomes

The pathological results showed that 32 patients (28.8%) achieved pCR (pTRG: 0) (Supplementary Table 1). The relationship between mrTRG and pTRG is presented in Table 3. Before nCRT, K_{trans} in the pCR group was significantly higher than in the non-pCR group, but there was no significant difference in K_{ep} or V_e between the two groups. After treatment, there was no significant difference in the above parameters between the two groups (Table 2 and Figure 1). Univariate logistic regression was performed to investigate the relationship between the mrTRG grading, post-treatment ADC value, and pathological outcomes. The results suggested that mrTRG grade 3 patients had a significantly lower probability of achieving pCR compared with grade 1 patients ($B = -2.56$, $P = 0.032$). The post-treatment ADC value was significantly correlated with the outcome ($B = 4.91$, $P < 0.001$).

Predictive performance of golden-angle radial sparse parallel dynamic contrast-enhanced magnetic resonance imaging parameters for pathological complete response

According to the ROC curve analyses, the area under the curve (AUC) of mrTRG (level 1–2), average ADC value (optimal threshold 1.05 × 10^{-3} mm^2), and K_{trans} value (optimal threshold 0.95/min) for predicting pCR were 0.738 (95% CI: 0.646–0.817), 0.782 (95% CI: 0.692–0.855), and 0.844 (95% CI: 0.772–0.916), respectively. The model combining the three parameters had the highest AUC (0.942, 95% CI: 0.881–0.977) (Figure 3 and Table 4). The DeLong test showed that the ability of the model to predict pCR when combining all three parameters was better than that of mrTRG, ADC value, and K_{trans} value alone ($P = 0.015$, 0.023, and 0.030, respectively) but not better than the model combining mrTRG and K_{trans} ($P = 0.099$).

Discussion

In the current study, we investigated the use of GRASP DCE-MRI for predicting pCR in patients with RC who underwent nCRT. The parameters (mrTRG, ADC, and K_{trans}) obtained from GRASP DCE-MRI imaging were used to quantify the predictive ability of the technique. Our results demonstrated that GRASP DCE-MRI imaging can predict pCR well. The predictive ability of the model combining the three parameters was ideal, with an AUC as high as 0.942. To the best of our knowledge, this is the first study to explore the role of GRASP DCE-MRI in predicting pCR for patients with RC.

For evaluating the efficacy of nCRT, MRI has the advantage of being non-invasive, and the mrTRG is a reliable parameter to evaluate the efficacy of nCRT.[24,25] However, the accuracy of mrTRG has been contested. Tumor re-

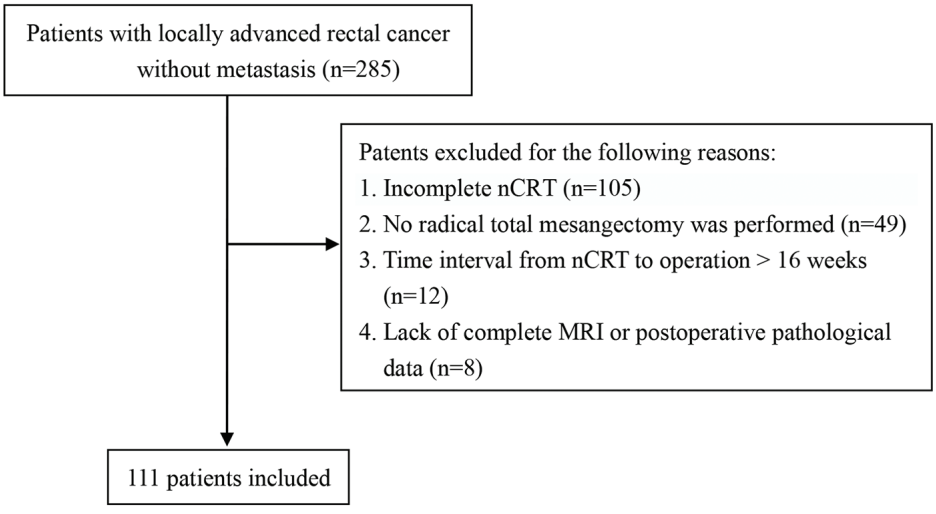

Figure 2. Patient selection flowchart. nCRT, neoadjuvant chemoradiotherapy; MRI, magnetic resonance imaging.

Table 2. Comparison of GRASP DCE-MR parameters before and after nCRT in pCR and non-pCR group

Group	Overall (n = 111)			pCR (n = 32)			Non-pCR (n = 79)		
	K_{trans} (/min)	K_{ep} (/min)	V_e	K_{trans} (/min)	K_{ep} (/min)	V_e	K_{trans} (/min)	K_{ep} (/min)	V_e
Pre-treatment (mean ± SD)	0.96 ± 0.40	0.69 ± 0.54	0.59 ± 0.36	1.30 ± 0.24	1.49 ± 0.39	0.57 ± 0.22	0.88 ± 0.34	1.37 ± 0.34	0.47 ± 0.23
Post-treatment (mean ± SD)	0.44 ± 0.25	0.55 ± 0.38	0.54 ± 0.26	0.55 ± 0.38	0.54 ± 0.26	0.35 ± 0.18	0.43 ± 0.25	0.75 ± 0.25	0.38 ± 0.27
t value	10.36	12.04	1.55	7.56	1.4	1.91	0.84	1.65	0.44
P value	<0.001	0.02	0.12	<0.001	0.08	0.06	0.40	0.10	0.67

nCRT, neoadjuvant chemoradiotherapy; K_{trans}, volume transfer constant; K_{ep}, rate constant; V_e, extracellular extravascular space volume fraction; pCR, complete response according to pathological outcome; GRASP, golden-angle radial sparse parallel; DCE-MR, dynamic contrast-enhanced magnetic resonance; SD, standard deviation.

Table 3. Relationship between mrTRG and pTRG after nCRT

mrTRG	pTRG					
	Grade 0	Grade 1	Grade 2	Grade 3	Grade 4	In total
Grade 1	5	0	0	0	0	5
Grade 2	16	1	0	1	0	18
Grade 3	11	28	28	1	0	68
Grade 4	0	0	2	15	0	17
Grade 5	0	1	0	2	0	3
In total	32	30	30	19	0	111

TRG, tumor regression grading; pTRG, TRG according to pathological outcomes; mrTRG, TRG according to magnetic resonance imaging evaluations; nCRT, neoadjuvant chemoradiotherapy.

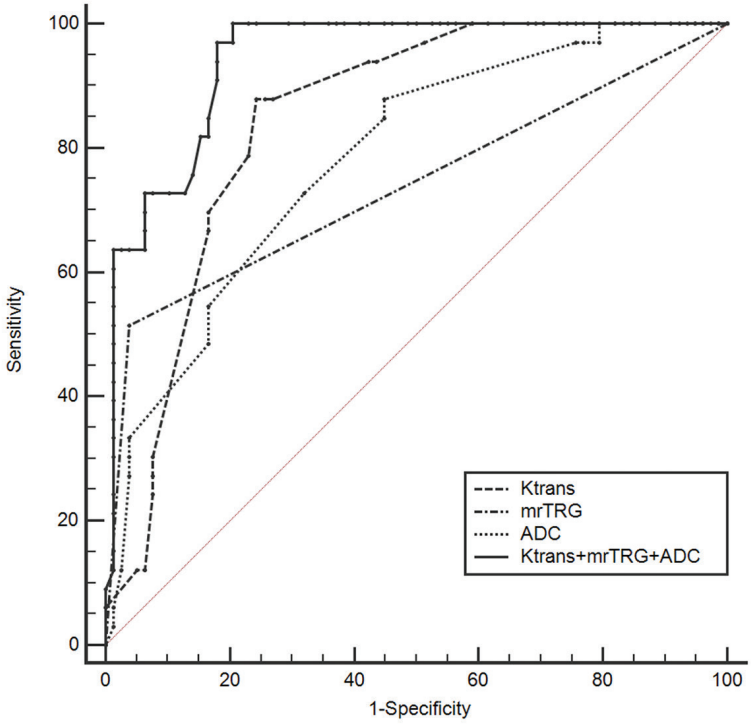

Figure 3. Ability of the magnetic resonance imaging-based tumor regression grading, apparent diffusion coefficient, and perfusion parameter in predicting pathological complete response after neoadjuvant chemoradiotherapy for rectal cancer.

gression after nCRT is a continuous process, with the peak usually occurring 8–11 weeks after the completion of treatment. This may explain the difference between mrTRG and pTRG.[26] In this study, MRI was performed 8 weeks after nCRT, and the median interval between MRI and radical surgery was 1 week. The sensitivity of mrTRG (71.5%) in our study was comparable with that (74.4%) reported by Sclafani et al.[27] In that study, the median interval between MRI and surgery was 2.7 weeks. There is still no evidence to standardize the selection of MR examination and operation time, and its influence on pCR prediction results is still unknown. Therefore, further studies are required to clarify this aspect.

However, this study defined mrTRG1–2 as cCR, and the sensitivity of mrTRG1–2 in the study by Bhoday et al.[28] was 66.7%. If mrTRG3 is included in the category of cCR, its sensitivity is greatly improved to 94%. This would further enhance the value of GRASP DCE-MRI. Whether mrTRG3 can be defined as a cCR also needs further study. Moreover, our results showed that mrTRG had good specificity (96.2%) for pCR, suggesting a higher diagnostic ability of mrTRG for patients with poor therapeutic efficacy (pTRG 2–4 grade).

The post-nCRT occurrence of necrosis and fibrosis in the tumor results in a decrease in the T2WI signal. However, there may still be a small number of tumor cells in the scarred and fibrotic tissue, which is not accurately distinguished by mrTRG. The addition of DWI can evaluate residual tumor activity to compensate for the deficiency of mrTRG in pCR prediction.[29] The ADC value is a quantitative index of the DWI sequence, and its increase is related to tumor necrosis. In one study, the average ADC value in patients achieving pCR was significantly higher than that in patients

Table 4. Ability of ADC, mrTRG, K_{trans}, and combined models to predict pCR after nCRT

	ADC	mrTRG	K_{trans}	ADC + mrTRG	ADC + K_{trans}	mrTRG + K_{trans}	ADC + mrTRG + K_{trans}
AUC (95% CI)	0.782 (0.694–0.85)	0.738 (0.646–0.817)	0.844 (0.763–0.906)	0.877 (0.801–0.932)	0.893 (0.82–0.944)	0.919 (0.851–0.962)	0.942 (0.881–0.977)
P values for Delong test*	0.023	0.015	0.030	0.039	0.049	0.099	
Accuracy	0.775	0.829	0.784	0.82	0.784	0.848	0.865
Specificity	0.962	0.962	0.833	0.936	0.872	0.897	0.923
Sensitivity	0.733	0.715	0.667	0.546	0.576	0.697	0.727
Positive predictive value	0.686	0.85	0.629	0.783	0.655	0.742	0.8
Negative predictive value	0.773	0.824	0.855	0.83	0.829	0.875	0.889

*The Delong test results were obtained from the comparison results of the combined model (three parameters included) with other parameters or models. ADC, apparent diffusion coefficient; TRG, tumor regression grading; pCR, complete response according to pathological outcome; nCRT, neoadjuvant chemoradiotherapy; K_{trans}, volume transfer constant; mrTRG according to magnetic resonance evaluations; AUC, area under the curve; CI, confidence interval.

who did not.[30] However, another study by Chandramohan et al.[30] found no significant association between the ADC value and pCR,[31] which may be due to the small sample size in their study (n = 22). The present study had a larger sample size, and we observed that the ADC value was significantly correlated with the outcome (B = 4.91, P < 0.001). Furthermore, ROC curve analysis revealed a moderate predictive ability of ADC (AUC: 0.78).

In this study, the RESOLVE sequence is affiliated with readout-segmented echo-planar imaging (readout-RS-EPI). Readout RS-EPI is characterized by small deformation and high resolution, which has little influence on the generated ADC value, thus reducing the impact of ADC value measurement bias.[32] Factors such as mucin pools in tumors, tiny residual tumor cell nests, low spatial resolution of DWI, radiation proctitis, and intestinal wall fibrosis may limit the predictive ability of ADC.[30] Nine patients in this study showed mucoid changes after treatment, increasing the average ADC value; thus, false positives may occur.

Angiogenesis is essential for tumor growth. In this study, the K_{trans} value of patients in the pCR group was higher than that in the non-pCR group, suggesting that chemotherapy drugs were more likely to enter the blood vessels with high permeability, and the blood vessels with high permeability had better oxygenation capacity and radiosensitivity.[33] The K_{trans} and K_{ep} values showed a significant decrease after treatment, which may be related to CRT-induced tumor necrosis and interstitial fibrosis. In this study, the results showed a high specificity but suboptimal sensitivity of K_{trans} for predicting pCR. Therefore, the use of K_{trans} alone may have low accuracy in predicting pCR. In addition, there was no significant difference in K_{trans}, K_{ep}, or V_e between the pCR group and non-pCR group after treatment, which is similar to the study by Kim et al.[34] but differs from the study by Gollub al.[16] The difference in results may be related to the non-standard combined cytotoxic and anti-angiogenic nCRT regimen adopted by Gollub et al.[16], whereas the standard nCRT regimen was adopted in our cohort. It may also be related to the GRASP DCE-MRI acquisition adopted in this study, in which 21 spokes were combined in each image, resulting in a time resolution of 3.45 s. This single reconstruction is well-balanced because it has a sufficiently high spatial resolution to compute perfusion maps and morphological assessments.[19] The combined model (mrTRG + ADC + K_{trans}) had the highest ability in predicting pCR (AUC: 0.942). However, the predictive ability was not superior to that of the combination model (mrTRG + K_{trans}; P = 0.099). This may be related to the small tumor parenchyma of pCR patients, which is difficult to measure. Moreover, the measurement error of the ADC value discussed above may also play a role. However, due to the lack of more detailed criteria and interobserver agreement, the current evaluation results based on imaging modalities were not consistent among centers and showed poor reproducibility. The pTRG may still play an irreplaceable role in the evaluation of nCRT treatment efficacy for patients with RC.

Some limitations of this study should be considered when interpreting the results. First, the retrospective nature of the study may have introduced an element of selection bias. Second, tumor regression and diffusion limitation due to tissue edema, fibrosis, and radiation enteritis after treatment all cause difficulties and biases in the measurement of mrTRG, ADC, and GRASP DCE-MRI parameters. Finally, the change in ADC value before and after nCRT was not analyzed in this study due to the lack of data. The change in ADC value may be a more accurate predictor of pCR.

In conclusion, the results of this study indicated that for patients with LARC who underwent nCRT, the K_{trans} values obtained from GRASP DCE-MRI, mrTRG, and ADC can be used as non-invasive indicators to evaluate the treatment efficacy of nCRT, and adding the K_{trans} value to mrTRG and ADC can lead to a better pCR predictive performance. Our findings may help inform individualized treatment planning.

Conflict of interest disclosure

The authors declared no conflicts of interest.

Funding

This study was supported by the Ningbo Science and Technology Public Welfare Project (grant no: 2022S26, grant no: 2022S133), the HwaMei Research Foundation of Ningbo No. 2 Hospital (grant no.: 2023HMKY50), and the Ningbo Clinical Research Center for Medical Imaging (grant no: 2022LYKEYB03).

References

1. Sung H, Ferlay J, Siegel RL, et al. Global Cancer Statistics 2020: GLOBOCAN estimates of incidence and mortality worldwide for 36 cancers in 185 countries. *CA Cancer J Clin*. 2021;71(3):209-249. [CrossRef]
2. Siegel RL, Miller KD, Goding Sauer A, et al. Colorectal cancer statistics, 2020. *CA Cancer J Clin*. 2020;70(3):145-164. [CrossRef]
3. Valentini V, Aristei C, Glimelius B, et al. Multidisciplinary rectal cancer management: 2nd European Rectal Cancer Consensus Conference (EURECA-CC2). *Radiother Oncol*. 2009;92(2):148-163. [CrossRef]
4. Martin ST, Heneghan HM, Winter DC. Systematic review and meta-analysis of outcomes following pathological complete response to neoadjuvant chemoradiotherapy for rectal cancer. *Br J Surg*. 2012;99(7):918-928. [CrossRef]
5. de Campos-Lobato LF, Stocchi L, da Luz Moreira A, et al. Pathologic complete response after neoadjuvant treatment for rectal cancer decreases distant recurrence and could eradicate local recurrence. *Ann Surg Oncol*. 2011;18(6):1590-1598. [CrossRef]
6. Bedrosian I, Rodriguez-Bigas MA, Feig B, et al. Predicting the node-negative mesorectum after preoperative chemoradiation for locally advanced rectal carcinoma. *J Gastrointest Surg*. 2004;8(1):62-63. [CrossRef]
7. Habr-Gama A, Perez RO, Nadalin W, et al. Operative versus nonoperative treatment for stage 0 distal rectal cancer following chemoradiation therapy: long-term results. *Ann Surg*. 2004;240(4):717-718. [CrossRef]
8. Renehan AG, Malcomson L, Emsley R, et al. Watch-and-wait approach versus surgical resection after chemoradiotherapy for patients with rectal cancer (the OnCoRe project): a propensity-score matched cohort analysis. *Lancet Oncol*. 2016;17(2):174-183. [CrossRef]
9. Rullier E, Vendrely V, Asselineau J, et al. Organ preservation with chemoradiotherapy plus local excision for rectal cancer: 5-year results of the GRECCAR 2 randomised trial. *Lancet Gastroenterol Hepatol*. 2020;5(5):465-474. [CrossRef]
10. Patel UB, Taylor F, Blomqvist, et al. Magnetic resonance imaging-detected tumor response for locally advanced rectal cancer predicts survival outcomes: MERCURY experience. *J Clin Oncol*. 2011;29(28):3753-3760. [CrossRef]
11. Dresen RC, Beets GL, Rutten HJ, et al. Locally advanced rectal cancer: MR imaging for restaging after neoadjuvant radiation therapy with concomitant chemotherapy. Part I. Are we able to predict tumor confined to the rectal wall? *Radiology*. 2009;252(1):71-80. [CrossRef]
12. Pham TT, Liney GP, Wong K, Barton MB. Functional MRI for quantitative treatment response prediction in locally advanced rectal cancer. *Br J Radiol*. 2017;90(1072):20151078. [CrossRef]

13. Memon S, Lynch AC, Bressel M, Wise AG, Heriot AG. Systematic review and meta-analysis of the accuracy of MRI and endorectal ultrasound in the restaging and response assessment of rectal cancer following neoadjuvant therapy. *Colorectal Dis*. 2015;17(9):748-761. [CrossRef]
14. Just N. Improving tumour heterogeneity MRI assessment with histograms. *Br J Cancer*. 2014;111(12):2205-2213. [CrossRef]
15. Li Z, Huang H, Wang C, et al. DCE-MRI radiomics models predicting the expression of radioresistant-related factors of LRP-1 and survivin in locally advanced rectal cancer. *Front Oncol*. 2022;12881341. [CrossRef]
16. Gollub MJ, Gultekin DH, Akin O, et al. Dynamic contrast enhanced-MRI for the detection of pathological complete response to neoadjuvant chemotherapy for locally advanced rectal cancer. *Eur Radiol*. 2012;22(4):821-831. [CrossRef]
17. Kim SH, Lee JM, Gupta SN, Han JK, Choi BI. Dynamic contrast-enhanced MRI to evaluate the therapeutic response to neoadjuvant chemoradiation therapy in locally advanced rectal cancer. *J Magn Reson Imaging*. 2014;40(3):730-737. [CrossRef]
18. Fusco R, Granata V, Sansone M, et al. Validation of the standardized index of shape tool to analyze DCE-MRI data in the assessment of neo-adjuvant therapy in locally advanced rectal cancer. *Radiol Med*. 2021;126(8):1044-1054. [CrossRef]
19. Attenberger UI, Liu J, Riffel P, et al. Quantitative perfusion analysis of the rectum using golden-angle radial sparse parallel magnetic resonance imaging: initial experience and comparison to time-resolved angiography with interleaved stochastic trajectories. I*nvest Radiol*. 2017;52(12):715-724. [CrossRef]
20. Riffel P, Zoellner FG, Budjan J, et al. "One-Stop Shop": free-breathing dynamic contrast-enhanced magnetic resonance imaging of the kidney using iterative reconstruction and continuous golden-angle radial sampling. *Invest Radiol*. 2016;51(11):714-719. [CrossRef]
21. Feng L, Grimm R, Block KT, et al. Golden-angle radial sparse parallel MRI: combination of compressed sensing, parallel imaging, and golden-angle radial sampling for fast and flexible dynamic volumetric MRI. *Magn Reson Med*. 2014;72(3):707-717. [CrossRef]
22. Rosenkrantz AB, Geppert C, Grimm R, et al. Dynamic contrast-enhanced MRI of the prostate with high spatiotemporal resolution using compressed sensing, parallel imaging, and continuous golden-angle radial sampling: preliminary experience. *J Magn Reson Imaging*. 2015;41(5):1365-1373. [CrossRef]
23. Mandard AM, Dalibard F, Mandard JC, et al. Pathologic assessment of tumor regression after preoperative chemoradiotherapy of esophageal carcinoma. Clinicopathologic correlations. *Cancer*. 1994;73(11):2680-2686. [CrossRef]
24. Tan Z, Cheng L, Xie L, et al. Comparison of the diagnostic performance of changes in signal intensity and volume from multiparametric MRI for assessing response of rectal cancer to neoadjuvant chemoradiotherapy. *Asia Pac J Clin Oncol*. 2023;19(3):327-336. [CrossRef]
25. Boubaddi M, Fleming C, Vendrely V, et al. Feasibility study of a response surveillance program in locally advanced mid and low rectal cancer to increase organ preservation. *Eur J Surg Oncol*. 2023;49(1):237-243. [CrossRef]
26. Sun Z, Adam MA, Kim J, Shenoi M, Migaly J, Mantyh CR. Optimal timing to surgery after neoadjuvant chemoradiotherapy for locally advanced rectal cancer. Optimal timing to surgery after neoadjuvant chemoradiotherapy for locally advanced rectal cancer. *J Am Coll Surg*. 2016;222(4):367-374. [CrossRef]
27. Sclafani F, Brown G, Cunningham D, et al. Comparison between MRI and pathology in the assessment of tumour regression grade in rectal cancer. *Br J Cancer*. 2017;117(10):1478-1485. [CrossRef]
28. Bhoday J, Smith F, Siddiqui MR, et al. Magnetic resonance tumor regression grade and residual mucosal abnormality as predictors for pathological complete response in rectal cancer postneoadjuvant chemoradiotherapy. *Dis Colon Rectum*. 2016;59(10):925-933. [CrossRef]
29. Horvat N, Veeraraghavan H, Khan M, et al. MR Imaging of rectal cancer: radiomics analysis to assess treatment response after neoadjuvant therapy. *Radiology*. 2018;287(3):833-843. [CrossRef]
30. Chandramohan A, Siddiqi UM, Mittal R, et al. Diffusion weighted imaging improves diagnostic ability of MRI for determining complete response to neoadjuvant therapy in locally advanced rectal cancer. *Eur J Radiol Open*. 2020;7100223. [CrossRef]
31. Jacobs L, Intven M, van Lelyveld N, et al. Diffusion-weighted MRI for early prediction of treatment response on preoperative chemoradiotherapy for patients with locally advanced rectal cancer: a feasibility study. *Ann Surg*. 2016;263(3):522-528. [CrossRef]
32. Tang C, Lin MB, Xu JL, et al. Are ADC values of readout-segmented echo-planar diffusion-weighted imaging (RESOLVE) correlated with pathological prognostic factors in rectal adenocarcinoma? *World J Surg Oncol*. 2018;16(1):138. [CrossRef]
33. Cooper RA, Carrington BM, Loncaster JA, et al. Tumour oxygenation levels correlate with dynamic contrast-enhanced magnetic resonance imaging parameters in carcinoma of the cervix. *Radiother Oncol*. 2000;57(1):53-59. [CrossRef]
34. Kim SH, Lee JM, Hong SH, et al. Locally advanced rectal cancer: added value of diffusion-weighted MR imaging in the evaluation of tumor response to neoadjuvant chemo- and radiation therapy. *Radiology*. 2009;253(1):116-125. [CrossRef]

Supplementary Table 1. Parameters for MRI scans

Parameters	T2 weighted imaging	Resolve DWI	Grasp DCE-MRI
Plane	Axial position (perpendicular to the long axis of the tumor)	Axial position	Axial position
Repeat time/echo time (ms)	6770/104	5800/78	4.09/1.95
Number of layer	35	35	24
Layer thickness (mm)	3	3	3
Layer distance (mm)	0.6	0.6	0.6
Field of view (mm)	220 x 220	220 x 220	240 x 240
Matrix of scanning	384 x 384	114 x 114	256 x 256
Pixel	0.33 x 0.33 x 3.0	1.0 x 1.0 x 3.0	0.9 x 0.9 x 3.0
Fat inhibition	No	Yes	Yes
B value (s)	-	0,50,1000	-
GRAPPA acceleration factor	1	1	1
Acquisition time	2 min 15s	3 min 13s	6 min 06s

MRI, magnetic resonance imaging; DWI, diffusion weighted imaging; Grasp DCE-MRI, Golden-angle radial sparse parallel dynamic contrast-enhanced magnetic resonance imaging.